Reaction Mechanism Study of the Di-Air System and Selectivity and Reactivity of NO Reduction in Excess O_2

Makkee, Michiel; Wang, Yixiao

DOI
10.4271/2017-01-0910

Publication date
2017

Document Version
Accepted author manuscript

Published in
SAE International Journal of Engines

Reaction mechanism study of the Di-Air system and selectivity and reactivity of NO reduction in excess O_2

Author, co-author (Do NOT enter this information. It will be pulled from participant tab in MyTechZone)

Affiliation (Do NOT enter this information. It will be pulled from participant tab in MyTechZone)

Abstract

We studied the mechanism of NO reduction as well as its selectivity and reactivity in the presence of excess O_2. Results show that fuel injection and/or pretreatment are important for ceria catalyst reduction and carbon deposition on the catalyst surface. Oxygen defects of reduced ceria are the key sites for the reduction of NO into N_2. The deposited carbon acts as a buffer reductant, *i.e.*, the oxidation of carbon by lattice oxygen recreates oxygen defects to extend the NO reduction time interval. A small amount of NO showed a full conversion into only N_2 both on the reduced Zr-La doped ceria and reduced Pt-Zr-La doped ceria. Only when the catalyst is oxidised NO is converted into NO_2.

1. Introduction

A mandatory introduction of a CO_2 emission target of 95 g/km by the year 2020 in the EU for automotive manufactures drives the development of increasingly fuel efficient cars. The requirement of the current Euro 6 emission standard has led to the development of highly efficient lean burn turbo-charged engines and catalytic deNO_x systems (Lean NO_x Traps (NSR) for gasoline engines and Urea-Selective Catalytic reduction (SCR) and or a combination of SCR and NSR for diesel engines). Euro 7 (or EURO 6B and 6C) requires a further reduction of the NO_x emissions from 0.18 g/km (Euro 5) via 0.08 g/km (Euro 6) to 0.04 g/km, while particulate matter emissions remain at 0.0045 g/km. Currently, the amount of NO emission, tested in the laboratory, does not reflect the amount emitted during the real driving conditions [1-3]. As of September 2017, the European Commission will proclaim that the real driving emission (RDE) will partially replace the current laboratory test in order to introduce new car models into the market [4]. These new regulation means that the tested cars will be driven outside on a real road under conditions of acceleration and deceleration that are beyond the current laboratory testing procedures. The pollutant emissions will be measured by portable emission measuring systems (PEMS). The RDE testing is expected to reduce the current difference of the pollutant emissions between laboratory and road.

Up to 2.1 times NO_x emission (0.168 g/km), relatively to the current Euro 6 NO_x emission standard (0.08 g/km), is allowed under the RDE testing by September 2017 [4]. This highly indicated that current available technologies: Three-way catalyst (TWC) [5-7], Urea-SCR (Selective Catalytic Reduction) [8-10], Lean NO_x Traps (NSR) [11-13] and combination thereof still need to be significantly improved since almost all Euro 6 certified diesel cars in the RDE testing emitted on average 8 times higher than the current NOx emission standard [1-3] In future, the NO_x emission will become more and more stringent. Therefore, effective exhaust emissions after-treatment technologies will be needed.

Recently, Bisaiji *et al*. (Toyota Motor Company) developed the Di-Air system in which short fuel rich and long fuel lean periods are created by the directly injecting hydrocarbons (HC's) at a high frequency downstream of the engine in the exhaust system upstream of a NSR catalyst ($Pt/Rh/Ba/K/Ce/Al_2O_3$)[14]. The Di-Air system is promising to meet the future NO_x emission standards under real driving test conditions. Compared to the current NSR system's narrow operating temperature window, caused by the requirement to store the NO_x as nitrite/nitrate on the Ba component, the Di-Air system retains a high NO_x conversion (above 80%) up to 800 ^oC at a high space velocity up to $1.2 \cdot 10^5$ l/l/h. They found that HC's injection was more effective in the NO_x reduction in comparison to that of CO and H_2 [14, 15]. The unique performance of the Di-Air system was attributed to the formation of stable isocyanate (CNO) and isocyanide (CN) intermediates on the catalyst surface as being evidenced by FTIR observations [16]. However, CN and CNO species were observed at a low temperature (200 °C) and their intensities decreased as the temperature increased. The CN and CNO species were hardly detected at 600 °C. The high NO reduction efficiency at high temperatures in Di-Air system as reported can be difficult to relate to these CN and CNO species.

A different explanation can be conceived to explain the performance of the Di-Air system. In the 1990's Illán-Gômez *et al.* [17, 18] reported that activated carbon is active in NO_x reduction in a temperature window between 400 and 500 °C. A large fuel injection upstream of a catalyst bed might promote the carbon formation and this in turn might enhance the NO_x reduction. Another explanation can be that the reduced catalyst sites reduce NO_x directly, while the formed adsorbed hydrocarbon fragments and carbon deposits act as an oxygen scavenger under lean conditions.

The working principle of the Di-Air system has not been clearly illustrated by the inventor (Toyota), academia, or industry, making it difficult to further optimise the system for real application due to the lack of fundamental understanding and reasoning. In order to test the aforementioned alternative explanations, we initiated a detailed investigation into the operating principle of the Di-Air. The TAP (Temporal Analysis of Products) technique (a vacuum pulse-response technique) was mainly utilised to investigate the mechanism of NO reduction and the role of each Di-Air catalyst component ($Pt/Rh/Ba/K/Ce/Al_2O_3$) [19]. In addition, a flow reactor (under an

atmosphere pressure) was used to mimic the NO reduction in the real operation system, *i.e.*, a small amount of NO in O_2. This study aims to unveil the mechanism of the NO reduction and the competition and the selectivity of the NO reduction in the presence of excess O_2.

2. Experimental

A commercially available Zr-La doped ceria (hereafter denoted as ceria) was obtained from Engelhard (now BASF). The BET surface area of ceria is 65 m^2/g, detailed characterisation was previously reported [19]. Pt/ceria was prepared via incipient wetness impregnation. Tetra-ammine platinum (II) nitrate was used as the precursor. Subsequently, the sample was dried at 110 °C overnight and calcined at 550 °C for 24 h. The loading of Pt is 0.5 wt%, measured by inductively coupled plasma-atomic emission spectroscopy (ICP).

Temporal Analysis of Products (TAP) was used for the mechanism study. TAP is a vacuum pulse-response technique. Reactant gas pulses are introduced to a small finite volume upstream of a packed catalyst bed. The introduced reactant and formed product(s) upon interaction with the catalyst diffuse through the packed catalyst bed until they leave the packed bed. The reactant and product(s) are recorded *versus* time (response) by a mass spectrometer, details of this set-up can be found elsewhere [19]. In the TAP experiments with ^{15}NO and $^{18}O_2$ pulses: 1) the catalyst was firstly oxidised using an O_2 pulse train; 2) secondly, a pre-reduction step with C_3H_6 pulses was performed until the effluent of the reactor remained constant.

In-situ Raman spectra (Renishaw, 2000) were recorded using a temperature controlled *in-situ* Raman cell (Linkam, THMS 600). Ten scans were collected for each spectrum in the 100-4000 cm^{-1} range using a continuous grating mode with a resolution of 4 cm^{-1} and scan time of 10 s. The spectrometer was calibrated daily using a silicon standard with a strong band at 520 cm^{-1}. The ceria was firstly pre-treated by C_3H_6 (1000 ppm in N_2, flow rate 200 mL/min) for 2 h. N_2 was used to flush the cell for 20 min. Subsequently, NO (1000 ppm NO in N_2, flow rate of 200 mL/min) was admitted to the cell.

A flow reactor was used to explore the reactivity and selectivity of NO in O_2. 200 mg catalyst was placed in a 6 mm inner-diameter quartz reactor tube. A feed composition of 0.2 % or 0.05% of NO and 5% of O_2 (with He for balance) was used with a space velocity of $6.7 \cdot 10^4$ l/l/h. The reactor effluent was online analysed by mass spectrometry (MS, Hiden Analytical, HPR-20 QIC) and infrared (IR) spectroscopy (Perkin–Elmer, Spectrum One). For IR analysis a gas cell with KBr windows with a path length of ~5 cm was used. The spectra were measured in a continuous mode using the Perkin-Elmer 'Time-Base' software between 4000-700 cm^{-1} wavenumbers with a spectral resolution of 8 cm^{-1} and an acquisition of 8 scans per spectrum, resulting in a time interval of 23 s between each displayed spectrum.

3. Results

3.1 Mechanism study

3.1.1 ^{15}NO and $^{18}O_2$ pulses over C_3H_6 reduced ceria in TAP

In order to mimic fuel injection in the Di-Air system, C_3H_6 is used as a model fuel to pre-treat the catalyst. Ceria was pre-treated (reduced) by C_3H_6 at 560 °C before ^{15}NO pulse experiment.

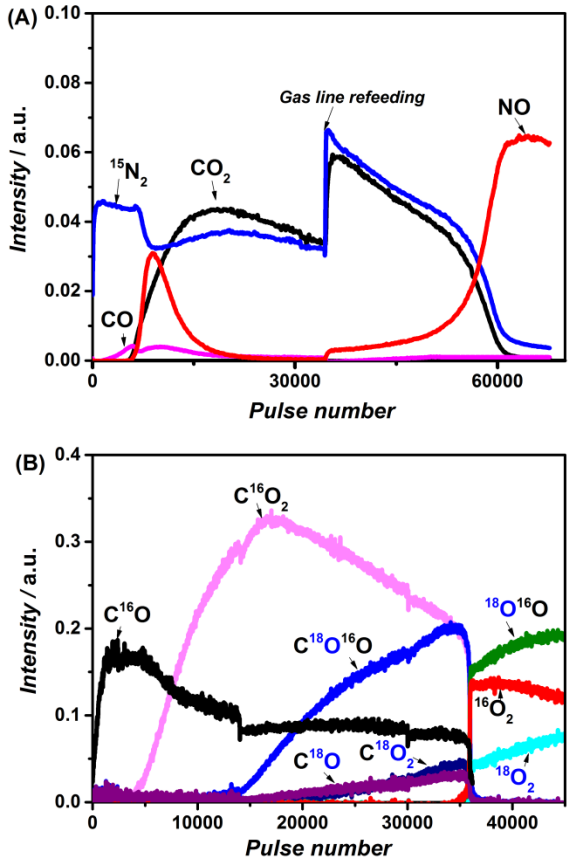

Figure 1. Reactant and product evolution upon pulsing (A) ^{15}NO at 560 °C and (B) $^{18}O_2$ at 530 °C over by C_3H_6 reduced ceria (21.2 mg) in TAP.

The pre-treatment of C_3H_6 resulted in $5.2 \cdot 10^{17}$ oxygen atoms / mg $_{Cat}$ extraction from the ceria lattice and $1.6 \cdot 10^{18}$ carbon atoms / mg $_{Cat}$ deposition on the ceria surface. Figure 1A showed the result of ^{15}NO pulses over C_3H_6 reduced ceria at 560 °C. The discontinuities in Figure 1A was attributed to the refilling of the ^{15}NO buffer vessel in the TAP. From 0 to 5340 pulses (Figure 1A), a full NO conversion was observed with $^{15}N_2$ as the main product (hardly any CO was formed). The evolution of CO_2 was observed from pulse number 5340 onwards. The evolution of CO_2 was closely followed by a temporary decrease in NO conversion. The NO conversion increased again from pulse number 8900. From pulse number 20000 to 35000, a full NO conversion was once again observed, while $^{15}N_2$ and CO_2 were the exclusive products. From pulse number 35000 till the end of the experiment, a progressive decrease to zero in NO conversion was observed. The N_2 and CO_2 production showed the same trend as the NO conversion. No or hardly any $^{15}N_2O$ or $^{15}NO_2$ were formed and no traces of -CN or -CNO were detected. In order to identify the oxygen species participating in the oxidation of deposited carbon after C_3H_6 pre-treatment, an $^{18}O_2$ pulse experiment over at 530 °C C_3H_6 reduced ceria was carried out. The pre-treatment of C_3H_6 led to approximately 2 hypothetical reduced ceria layers and 2-3 wt.% carbon deposition. Figure 1B showed the product evolution during the $^{18}O_2$ pulse experiment. The discontinuities in Figure 1B were at points where the $^{18}O_2$/He buffer vessel in the TAP was refilled. All introduced $^{18}O_2$ were completely converted until a steep oxygen breakthrough profile was observed from pulse number 35000. Exclusive $C^{16}O$ was evolved until pulse number 4000, where $C^{16}O_2$ started to form, and gradually became the dominant product. After

14000 pulses $C^{18}O^{16}O$ and $C^{18}O_2$ were observed. After 35000 pulses $C^{16}O$, $C^{16}O_2$, $C^{18}O^{16}O$, $C^{18}O$, and $C^{18}O_2$ decreased to zero, where $^{18}O_2$, $^{16}O_2$, and $^{18}O^{16}O$ started to breakthrough in a kind of exchange equilibrium. The observed $C^{18}O$ (m/e=30) was due to the fragmentation from $C^{18}O_2$ and $C^{18}O^{16}O$ and showed the same trend as the $C^{18}O_2$ and $C^{18}O^{16}O$ products. $^{18}O^{16}O$ was the main product after oxygen breakthrough.

3.1.2 *In-situ* Raman

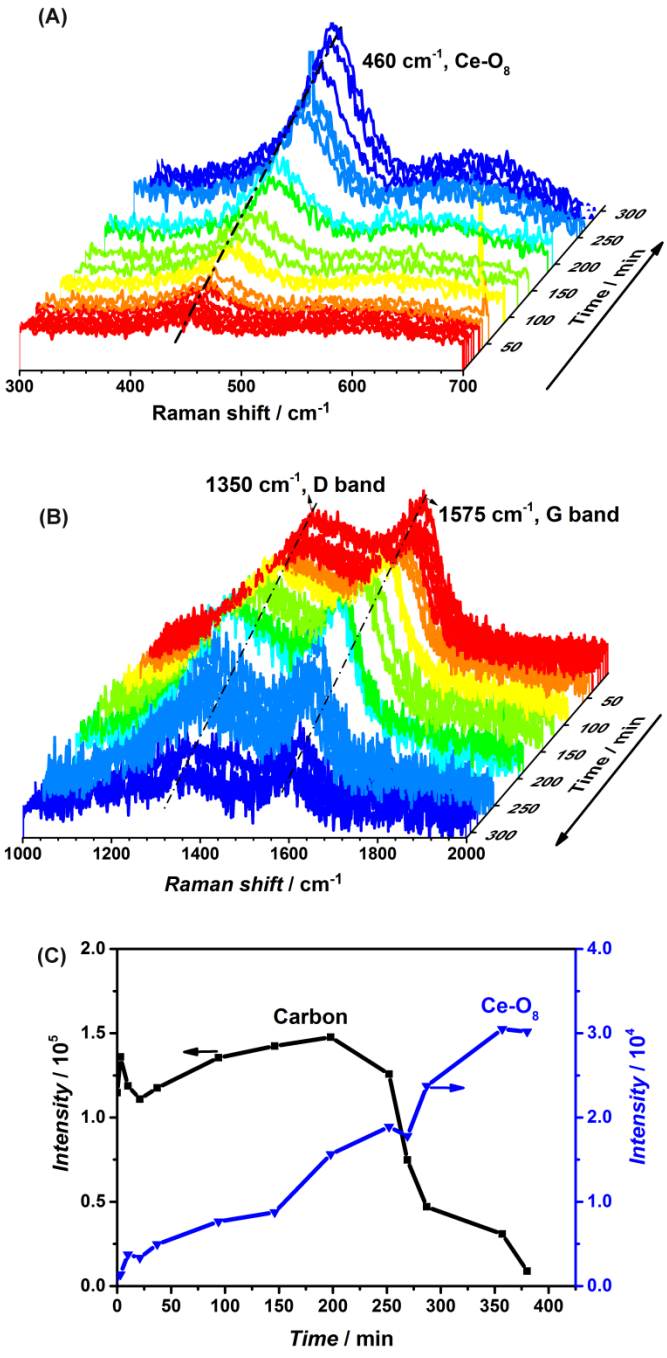

Figure 2. *In-situ Raman response for NO over at 560 °C C_3H_6 reduced ceria, Raman spectra of band at (A) 460 cm^{-1} and (B) 1575 and 1350 cm^{-1}; (C) Raman bands intensity of 460, 1575, and 1350 cm^{-1} responses versus time.*

Figure 2 showed *in-situ* Raman spectra for the NO reduction over at 560 °C C_3H_6 reduced ceria. The band at 460 cm^{-1} was attributed to the symmetric stretch mode of $Ce\text{-}O_8$ crystal unit, which was characteristic for the fluorite ceria structure [20]. The bands at 1575 and 1350 cm^{-1} were assigned to G band and D band of carbon in the form of graphene or graphite, respectively [21]. The G band was usually assigned to zone centre phonons of E_{2g} symmetry of the perfect graphite structure, and the D peak was a breathing mode of A_{1g} symmetry which was forbidden in a perfect graphite structure and only became active in the presence of structural defects and disorders. The band at 460 cm^{-1} was initially hardly visible and its intensity increased during the NO flow (Figure 2A and C). In contrast to the band at 460 cm^{-1} (Figure 2A and C), the band at 1575 and 1350 cm^{-1} had the same intensities during the NO flow and started to decrease after 200 min (Figure 2B and C).

3.1.3 ^{15}NO over C_3H_6 reduced Pt/ceria in TAP

Similarly to ceria, Pt/ceria was also pre-treated by C_3H_6. Instead of 560 °C, Pt/ceria pre-treatment with C_3H_6 was carried out at 450 °C, which was 110 °C lower than those of the experiments performed over bare ceria (Figure 1 and 2). The pre-treatment of C_3H_6 resulted in $6.3 \cdot 10^{17}$ oxygen atoms / mg $_{Cat}$ extraction from the ceria lattice and $2.8 \cdot 10^{17}$ carbon atoms / mg $_{Cat}$ deposition on the catalyst surface. Figure 3 showed the result of ^{15}NO pulse over at 450 °C C_3H_6 reduced Pt/ceria. From pulse number 0 to 1000 (Figure 3), full NO conversion was observed with $^{15}N_2$ as the main product (small amount of CO formed). The evolution of CO_2 was observed from pulse number 1000. Instead of a temporary decrease in NO conversion, NO showed full conversion until pulse number 4000, where $^{15}N_2$ and CO_2 were the only products. From pulse number 4000 onwards, a progressive decrease to zero for the NO conversion was observed. The N_2 and CO_2 production followed the same trend as the NO conversion. No or hardly any $^{15}N_2O$ or $^{15}NO_2$ were formed and no traces of -CN or -CNO were detected.

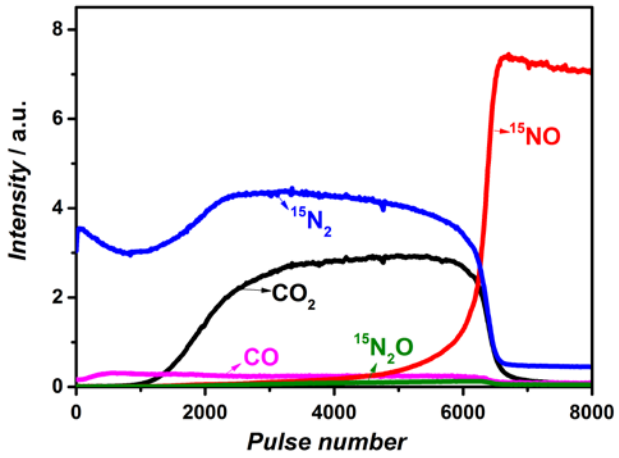

Figure 3. Reactant and product evolution upon pulsing ^{15}NO over at 450 °C C_3H_6 reduced Pt/ceria (10 mg).

3.2 NO reduction in O_2 over reduced ceria

Similarly to TAP experiments, C_3H_6 was also used as a model fuel in the flow reactor. The ceria was pre-treated with C_3H_6 (1.25% in N_2) for 2 h at 600 °C and subsequently (0.2% or 0.05%) NO and 5% O_2 (balance He) was admitted with a flow rate of 200 mL/min. The pre-

treatment of C_3H_6 resulted in $7.9\cdot10^{17}$ oxygen atoms / mg $_{Cat}$ extraction from the ceria lattice and $2\cdot10^{18}$ carbon atoms / mg $_{Cat}$ deposition on the ceria surface. Figure 4A showed the results of 0.2% NO + 5% O_2 over the reduced ceria. m/e= 28 and 44 were observed during the first 90 s. m/e=28 could be attributed to the CO and N_2. The formation of CO was confirmed from the IR spectra (Figure 5). N_2, however, was not able to be detected due to its IR inactivity. To prove the formation of N_2, 0.2% ^{15}NO + 5% O_2 over the reduced ceria were performed (not shown). The observation of $^{15}N_2$ (m/e=30) proved that the reduction of NO into N_2. m/e of 44 could be attributed to N_2O and CO_2. From the IR spectra (Figure 5), no N_2O was detected, indicating that the m/e=44 was originated from CO_2. Initially full NO and O_2 conversion and both started to breakthrough at 75 s and became stable after 100 s.

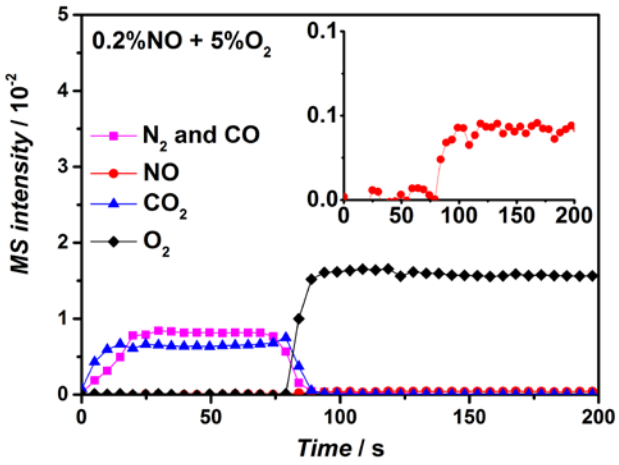

Figure 4. *Reactant and product evolution in flow reactor for 0.2 % NO + 5% O_2 over reduced ceria; inset is NO evolution.*

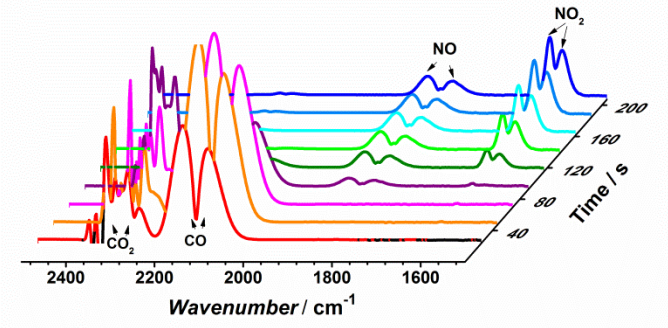

Figure 5. *IR spectra of 0.2 % NO + 5% O_2 over reduced ceria in flow reactor.*

Similarly to 0.2% NO+ 5% O_2 (Figure 4A), 0.05% NO + 5% O_2 over the reduced ceria C_3H_6 showed the formation of N_2, CO, and CO_2. Both NO and O_2 started to breakthrough at 75 s.

Figure 5 showed the IR spectra responses for 0.2% NO + 5% O_2 in helium over reduced ceria. The interval of IR spectra is 23 s. Initially peaks at 2174 and 2116 cm^{-1}, assigned to CO, were observed and these peaks vanished after 138 s. The broad band at 2350 cm^{-1} was assigned to CO_2 and followed the same trend in time as CO response. The peaks at 1601 and 1628 cm^{-1}, appearing from 116 s onwards, were attributed to the formation of NO_2. During the whole experiment, no N_2O was detected (IR peak intensity 2235 cm^{-1}, detection limit 1 ppm). Same IR responses were found for 0.05% NO + 5% O_2 experiment, both NO and NO_2 were observed from 93 s.

3.3 NO reduction in O_2 over reduced Pt/ceria

Similarly to ceria, the Pt/ceria was pre-treated with C_3H_6 (1.25% in N_2) for 2 h at 600 $^{\circ}C$ and subsequently (0.2% or 0.05%) NO and 5% O_2 (balance He) was admitted with a flow rate of 200 mL/min. The pre-treatment of C_3H_6 resulted in $9.8\cdot10^{17}$ oxygen atoms / mg $_{Cat}$ extraction from the ceria lattice and $1.7\cdot10^{18}$ carbon atoms / mg $_{Cat}$ deposition on the catalyst surface.

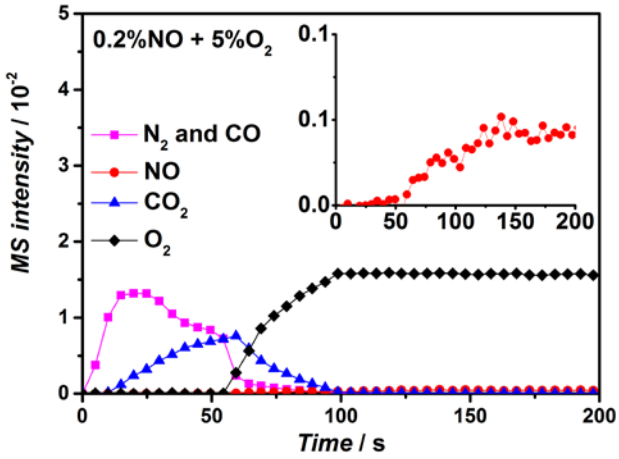

Figure 6. *Reactant and product evolution in flow reactor for 0.2 % NO + 5% O_2 over reduced Pt/ceria; inset is NO evolution .*

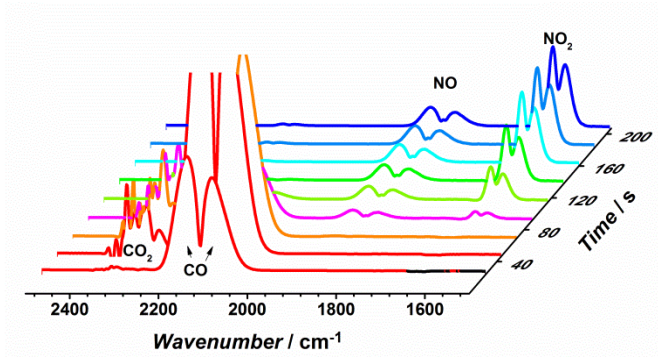

Figure 7. *IR spectra of 0.2 % NO + 5% O_2 over reduced Pt/ceria in flow reactor.*

Figure 6 showed the results of 0.2% NO + 5% O_2 over the reduced Pt/ceria. m/e= 28 and 44 were observed during the first 150 s. m/e=28 could be attributed to the CO and N_2. The formation of CO was confirmed from the IR spectra (Figure 7). N_2, however, was not able to be detected due to its IR inactivity. To prove the formation of N_2, 0.2% ^{15}NO + 5% O_2 over the reduced ceria were performed (not shown). The observation of $^{15}N_2$ (m/e=30) proved that the reduction of NO into N_2. m/e of 44 could be attributed to N_2O and CO_2. From the IR spectra (Figure 5), no N_2O was detected, indicating that the m/e=44 originated from CO_2. NO showed full conversion until 55 s and reached a stable signal from 150 s.

Similarly to 0.2% NO+ 5% O_2 (Figure 4), 0.05% NO + 5% O_2 over the reduced Pt/ceria C_3H_6 showed the formation of N_2, CO, and CO_2. Both NO and O_2 started to breakthrough at 55 s and reached stable signals from 150 s and 100 s, respectively.

Figure 7 showed the IR spectra responses for 0.2% NO + 5% O_2 in helium over reduced Pt/ceria. The interval of IR spectra is 23 s. Initially peaks at 2174 and 2116 cm^{-1}, assigned to CO, broad band at 2350 cm^{-1}, assigned to CO_2) were observed and these peaks vanished after 105 s. The peaks at 1601 and 1628 cm^{-1}, appearing from 85 s onwards, were attributed to the formation of NO_2. During the whole experiment, no N_2O was detected (IR peak intensity 2235 cm^{-1}, detection limit 1 ppm). Same IR responses were found for 0.05% NO + 5% O_2 experiment, both NO and NO_2 were observed from 93 s. Same IR responses were found for 0.05% NO + 5% O_2 experiment, both NO and NO_2 were observed from 105 s.

4. Discussion

4.1 Mechanism study

High frequency fuel injection was applied in the Di-Air system. To mimic this Di-Air system in the present study, the catalyst was pre-treated by C_3H_6 before NO reduction experiments. In order to distinguish N_2 and CO (m/e= 28) as well as CO_2 and N_2O (m/e=44), ^{15}NO was used to replace ^{14}NO.

Starting with the ceria, full NO conversion was observed from pulse number 0 to 5000 with exclusive formation of $^{15}N_2$ as shown in Figure 1A. The absence of oxidation products CO and CO_2 before pulse number 5000 indicated that the carbonaceous residues, left on the surface after C_3H_6 pre-reduction, did not directly participate in the reduction of ^{15}NO to $^{15}N_2$. A mechanism of direct dissociation of adsorbed NO on oxygen anion defect centres, in which the O side of NO filled the oxygen anion vacancy, and the N species recombined to form N_2 can explain the observation.

NO dissociated on oxygen anion defect centers of ceria, which was also found for the H_2 and CO reduction pre-treatment [19, 22]. NO dissociation resulted in a progressive re-oxidation of the catalyst with increasing NO pulse number, thereby decreasing the number of oxygen anion defect sites. When ceria is partially re-oxidised, CO_2 formation is observed, indicating that ceria became active in the oxidation of these deposited carbonaceous residues at a specific ceria oxidation state. The oxidation of carbonaceous deposits to each CO_2 molecule created two oxygen anion defect centres, forming one N_2 molecule from 2 NO molecules. This delayed CO_2 formation will inhibited the refilling of oxygen anion defect centers and cause a temporary decline in the NO conversion.

To support the role of lattice oxygen in the oxidation of deposited carbon, *i.e.*, gas-phase NO did not directly participate in the carbon deposit oxidation reaction, $^{18}O_2$ was pulsed over at 530 °C C_3H_6 reduced ceria, as shown in Figure 1B. The initial exclusive formation of $C^{16}O$ and $C^{16}O_2$ indicated that gas-phase oxygen was not directly involved in the oxidation of the carbon deposits, which was in agreement with previous findings in diesel soot on ceria based catalysts [23]. In summary, NO re-oxidised reduced ceria and was not directly involved in carbonaceous deposits oxidation. The oxidation of carbonaceous deposits to CO_2 by oxygen species originating from the lattice oxygen, will recreate oxygen anion defect centers, which were accountable for additional NO dissociation. Therefore, these carbonaceous deposits could be seen as a delayed or stored reductant.

Since TAP is an ultra-vacuum technique, *in-situ* Raman (at atmospheric pressure) was applied to confirm the results obtained from TAP. NO reduction into N_2 was performed over at 560 °C C_3H_6 reduced ceria, as shown in Figure 2. The band at 460 cm^{-1} (Figure 2A) was attributed to the symmetric stretch mode of the $Ce-O_8$ crystal unit, which was characteristic for reduced fluorite ceria structure [20]. This peak disappeared during the C_3H_6 pre-treatment, while it re-appeared under NO. This indicated that the reduced ceria was re-oxidised during NO flow. The bands at 1575 and 1350 cm^{-1} were assigned to G band and D band of carbon in the form of graphene or graphite (Figure 2B) and they remained constant during the first 200 min of NO in N_2 flow (Figure 2C). The change of the bands' intensity during NO flow indicated that the oxidation of carbon commenced later than the re-oxidation of ceria. This confirmed the TAP's finding: NO firstly re-oxidised oxygen defects in the reduced ceria and subsequently the oxidation of carbon started when ceria was largely oxidised.

Ceria is a vital ingredient in the Di-air catalyst and oxidises hydrocarbons and reduces NO into N_2. However, high temperatures (above 500 °C) were necessary to oxidise C_3H_6/C_3H_8. To successfully use ceria based catalysts, promotors might be beneficial to convert hydrocarbons at lower temperatures, thereby, a (deeper and faster) reduction of the ceria with a larger carbon deposits pool.

To lower the hydrocarbon activation, Pt was loaded on ceria and it significantly increased the C_3H_6 reactivity. The reduction of Pt/ceria by C_3H_6 at 450 °C led to $6.3 \cdot 10^{17}$ oxygen atoms /mg $_{Cat}$ of extraction from ceria lattice, which was around $1 \cdot 10^{17}$ oxygen atoms/ mg $_{Cat}$ more than the reduction of ceria at 560 °C. However, the amount of deposited carbon was around $2.8 \cdot 10^{18}$ carbon atoms/ mg $_{Cat}$, which was around 10 times less than that over ceria pre-treated by C_3H_6 at 560 °C. Although less carbon atoms were deposited over the Pt/ceria at 450 °C, Pt/ceria was still active in C_3H_6 oxidation and ceria reduction, since bare ceria was hardly active in C_3H_6 oxidation at 450 °C.

Figure 3 showed the ^{15}NO pulses over Pt/ceria pre-treated by C_3H_6 at 450 °C. The absence of oxidation products CO and CO_2 before pulse number 1000, indicated that the carbonaceous residues, left on the surface after C_3H_6 pre-reduction, did not directly participate in the reduction of ^{15}NO into $^{15}N_2$. Carbon oxidation started from pulse number 1000. This indicated that the presence of Pt did not change the principle of NO reduction into N_2. Oxygen defects were still the key sites for NO reduction into N_2 and the deposited carbon acted as a buffer reductant.

4.2 Competition of NO with O_2

For a typical diesel exhaust composition, approximately 200 ppm NO has to be reduced to 10 ppm NO in competition with an excess of 5% O_2, 5% CO_2, and 5-10% H_2O in order to meet the future automotive legislation emission standards. NO has to compete especially with O_2. O_2 is a strong oxidant and is also able to fill the oxygen defects of reduced ceria and oxidise deposited carbon. Although the results from TAP experiment showed that NO was able to be reduced on oxygen defect sites into N_2, it was still a question whether NO was able to reduce into N_2 in the presence of excess O_2. Therefore, 500 and 2000 ppm of NO was used to compete with 5% O_2 using reduced ceria and Pt/ceria.

As shown in the Figure 4A, the co-feeding 0.2% NO with 5% O_2 over reduced ceria led to the formation of CO, N_2, and CO_2 during

the first 75 s. Both NO and O_2 re-oxidised the oxygen defects. The formation of CO and CO_2 led to a consumption of the deposited carbons. NO and O_2 broke through simultaneously after 75 s and no conversion was found after 100 s. This indicated that NO was able to compete with O_2 for the oxygen defects although the NO concentration was 25 times lower than that of O_2. For 0.05% NO + 5% O_2, NO concentration was 100 times lower than that of O_2 and it was still able to compete with O_2 for oxygen defects,.

The same experiments were also performed over the Pt/ceria. As shown in the Figure 6, the co-feeding 0.2% NO with 5% O_2 resulted in the formation of N_2, CO, and CO_2. Compared the intensity of CO in Figure 4 and 6, more CO was formed over Pt/ceria than that in the case of ceria. The presence of Pt accelerated carbon oxidation reaction. In other words, the oxidation of carbon was more favorable to CO over the Pt/ceria than over ceria. This observation indicated that Pt accelerated the carbon oxidation and the diffusion of O via the ceria lattice became a rate limiting step. NO and O_2 broke through simultaneously after 55 s and no conversion observed after 100 s. This further indicated that NO could compete with O_2, since no NO was observed/detected (detection limit 1 ppm) in the process of ceria catalyst re-oxidation and deposited carbon oxidation.

The results in Figure 4 and 6 indicated that small amount of NO was able to compete with excess of O_2 over both Zr-La doped ceria and Pt/Zr-La doped ceria. The presence of Pt accelerated the carbon oxidation to CO, but did not alter the competition of NO with O_2.

4.3 Selectivity of NO reduction in O_2

Ceria can promote the oxidation of NO to NO_2 and, therefore, it is commonly used in the field of SCR-NH_3 and soot oxidation [24, 25]. Although NO showed full conversion during the 0.2% (and 0.05%) NO + 5% O_2 co-feeding over reduced ceria the first 75 s (Figure 4), the selectivity of NO reduction was more important than the reactivity. Undesired by-products, *i.e.*, N_2O and NO_2, were frequently reported in NOx abatement technologies.

The result of NO reduction in O_2 (Figure 4 and 6) showed that N_2O was not detected during the whole experiment. NO_2 was only formed when NO broke through in the gas phase. From the isotopic 0.2% ^{15}NO + 5% O_2, the formation of only $^{15}N_2$ in the first 75 s proved that N_2 was the exclusive product in the NO reduction into N_2 in O_2.

Pt is the preferred noble metal (catalyst) for the oxidation of NO into NO_2 for example in diesel soot oxidation [26]. Pt is commonly used in the NSR catalyst system and HC-SCR, which is regarded as the active site for the NO decomposition into N_2. Therefore, it will be a challenge to control the selectivity of NO conversion in the presence of O_2 to undesired by-products: N_2O and NO_2. To ascertain whether the addition of Pt to ceria could change the selectivity of NO into N_2, 0.2 % NO with 5% O_2 was fed to reduce Pt/ceria. Similarly to reduced ceria, NO in the presence of O_2 was reduced to N_2 over reduced Pt/ceria (Figure 4 and 6). No N_2O was observed in the whole experiment. NO_2 was only detected when NO broke through. From the 0.2% ^{15}NO + 5% O_2, the formation of $^{15}N_2$ in the first 55 s proved that N_2 was the exclusive product in the NO reduction to N_2 in the presence O_2. The results of Figure 5 and 7 indicated that the addition of Pt to ceria did not change the selectivity of NO to N_2.

The results in Figure 4-7 clearly demonstrated that the oxygen defects in reduced ceria were the active sites for the NO reduction. As long as ceria was reduced, NO was selectively converted to N_2. NO_2 was only formed when (Pt) ceria was completely re-oxidised.

5. Conclusions

Ceria is a promising starting material in the development of a Di-Air NOx abatement technology. Fuel injection directly into the catalyst will result in ceria reduction and carbon deposition. Oxygen defects on reduced ceria are responsible for NO decomposition into N_2, while carbon deposits will maintain a reduced ceria surface state, and, thereby, extend the effectiveness of the hydrocarbon injections (limit fuel penalty). Platinum lowers the reduction temperature of ceria and carbon deposition. Small amount of NO can completely compete with the excess of O_2 that no NO is detected during ceria re-oxidation and deposited carbon oxidation process. Moreover, NO is selectively reduced into N_2 in the presence of O_2 over reduced ceria and Pt/ceria. Only when (Pt) ceria is fully re-oxidised, NO will be converted into NO_2.

6. References

1. Carslaw, D.C., Beevers, S.D., Tate, J.E., Westmoreland, E.J. et al., Recent evidence concerning higher NO_x emissions from passenger cars and light duty vehicles, Atmospheric Environment, 2011. **45** (39)**:** p. 7053-7063.
2. Yang, L., Zhang, S., Wu, Y., Chen, Q., et al., Evaluating real-world CO_2 and NO_X emissions for public transit buses using a remote wireless on-board diagnostic (OBD) approach, Environmental Pollution, 2016.**218** : p. 453-462.
3. Real-World Exhaust Emissions from modern disel cars. http://www.theicct.org/sites/default/files/publications/ICCT_PEMS-study_diesel-cars_20141010.pdf
4. Commission welcomes Member States' agreement on robust testing of air pollution emissions by cars. http://europa.eu/rapid/press-release-IP-15-5945-en.htm
5. Miyoshi, N., Matsumoto, S.i., Katoh, K., Tanaka, T.et al. "Development of new concept three-way catalyst for automotive lean-burn engines," SAE Technical Paper 950809, 1995.
6. Rodrigues, F., Juste, L., Potvin, C., Tempere, J., et.al., "NO_x storage on barium-containing three-way catalyst in the presence of CO_2" Catalysis letters. 2001. **72**(1-2): p. 59-64.
7. Kim, G., "Ceria-promoted three-way catalysts for auto exhaust emission control," Industrial & Engineering Chemistry Product Research and Development, 1982. **21**(2): p. 267-274.
8. Koebel, M., Elsener, M., and Marti, T., "NO_x-reduction in diesel exhaust gas with urea and selective catalytic reduction," Combustion science and technology, 1996. **121**(1-6): p. 85-102.
9. Miller, W.R., Klein, J.T., Mueller, R., Doelling ,W., "The development of urea-SCR technology for US heavy duty trucks," SAE Technical Paper 2000-01-0190, 2000.
10. Hug, H., Mayer, A., and Hartenstein, A., "Off-highway exhaust gas after-treatment: Combining urea-SCR, oxidation catalysis and traps," SAE Technical Paper, 930363, 1993.
11. Matsumoto, S.I., "Recent advances in automobile exhaust catalyst," Catalysis Surveys from Asia, 1997. **1**(1): p. 111-117.
12. Ikeda, Y., Sobue, K., Tsuji, S., and Matsumoto, S.I., "Development of NO_x Storage-Reduction Three-way Catalyst for D-4 Engines,"SAE Technical Paper, 1999-01-1279, 1999.
13. Misono, M. and Inui, T., "New catalytic technologies in Japan," Catalysis today, 1999. **51**(3): p. 369-375.
14. Bisaiji, Y., Yoshida, K., Inoue, M., Umemoto, K., "Development of Di-Air-A New Diesel deNO_x System by Adsorbed

Intermediate Reductants," SAE International Journal of Fuels and Lubricants, 2012. **5**(1): p. 380-388.
15. Inoue, M., Bisaiji, Y., Yoshida, K., Takagi, N., "deNO_x Performance and Reaction Mechanism of the Di-Air System," Topics in Catalysis, 2013: p. 1-4.
16. Bisaiji, Y., Yoshida, K., Inoue, M., and Takagi N., "Reaction Mechanism Analysis of Di-Air-Contributions of Hydrocarbons and Intermediates," SAE International Journal of Fuels and Lubricants, 2012. **5** (2012-01-1744): p. 1310-1316.
17. Illán-Gómez, M.J., Raymundo-Piñero, E., García-García , A., Linares-Solano, A., "Catalytic NO_x reduction by carbon supporting metals," Applied Catalysis B: Environmental, 1999. **20**(4): p. 267-275.
18. Illán-Gómez, M.J., Linares-Solano, A., Radovic, L.R., and Salinas-Martínez de Lecea, C., "NO Reduction by Activated Carbons.Some Mechanistic Aspects of Uncatalyzed and Catalyzed Reaction," Energy & Fuels, 1996. **10**(1): p. 158-168.
19. Wang, Y., Posthuma de Boer, J., Kapteijn F., and Makkee, M., "Fundamental Understanding of the Di-Air System: The Role of Ceria in NO_x Abatement," Topics in Catalysis, 2016: p. 1-7.
20. Wang, Y., Posthuma de Boer, J., Kapteijn, F., and Makkee, M., "Next Generation Automotive deNO_x Catalysts: Ceria What Else?" ChemCatChem, 2016. **8**(1): p. 102-105.
21. Weber, W., Hass, K., and McBride, J., "Raman study of CeO_2: second-order scattering, lattice dynamics, and particle-size effects," Physical Review B, 1993. **48**(1): p. 178.
22. Ferrari, A., Meyer, J., Scardaci, V., Casiraghi, C., et al., "Raman spectrum of graphene and graphene layers," Physical review letters, 2006. **97**(18): p. 187401.
23. Bueno-López, A Krishna, K., Makkee, M., and Moulijn, J.A., "Enhanced soot oxidation by lattice oxygen via La^{3+}-doped CeO_2," Journal of Catalysis, 2005. **230**(1): p. 237-248.
24. Atribak, I., Azambre, B., López, A.B., and García-García, A., "Effect of NO_x adsorption/desorption over ceria-zirconia catalysts on the catalytic combustion of model soot," Applied Catalysis B: Environmental, 2009. **92**(1): p. 126-137.
25. Wu, Z., Jin R., Liu Y., and Wang, H.,"Ceria modified MnO_x/TiO_2 as a superior catalyst for NO reduction with NH_3 at low-temperature," Catalysis Communications, 2008. **9**(13): p. 2217-2220.
26. Krishna, K., Bueno-Lopez A., Makkee M., and Moulijn, J.A., "Potential rare-earth modified CeO_2 catalysts for soot oxidation part II: Characterisation and catalytic activity with $NO+O_2$,". Applied Catalysis B-Environmental, 2007. **75**(3-4): p. 201-209.

Contact Information

Prof.dr.ir. Michiel Makkee, Section Catalyis Engineering, Deaprtment Chemcial Engineering, Faculty Applied Sciences, Delft University of Technology, Julianalaan 136, NL 2628 BL Delft, The Netherlands, e-mail address: m.makkee@tudelft.nl

Acknowledgments

The authors acknowledge the China Scholarship Council (CSC) for financial support, Ramon Oord and Bert Weckhuysen (Inorganic Chemistry and Catalysis group, Debye Institute for Nanomaterials Science, Utrecht University) for their helpful assistance in performing De-NO_x flow reactor in Utrecht University, Daniël van den Berg and Yueting Liu for their scientific involvement and discussions.